Fengyu XU[1], Guoping JIANG[1]

College of Automation, Nanjing University of Posts and Telecommunications (1)

Climbing Robot Modelling Based on Grab Claws

Abstract. Though the wall-climbing robots have be used extensively, however, no effective adhesion system has been designed for robots deployed in high-altitude, rough concrete buildings that are subjected to large wind loads and vibrations. Therefore, an initial design of a wall-climbing robot based on grab claw is presented and a climbing model is proposed in the paper. The mathematical model is established to reflect the relations between sharp hook and the micro-protuberance on the rough wall surface The stress on the hook-like claws is analyzed under three different conditions, so the steady grasping condition of the hook-like claws is obtained. Simulation results are carried out which demonstrates the stability of the grasping. Finally, the system outline and field implement scheme are presented.

Streszczenie. W artykule przedstawiono projekt wspinającego się robota, opartego na chwytaku w postaci pazura. Zaproponowano także matematyczny model wspinania, pozwalający określić wpływ mikro-fałd na powierzchni pionowej na możliwość chwytania hakiem. Przeanalizowano możliwości obciążenia haka w trzech różnych warunkach pracy. Przeprowadzono badania symulacyjne i eksperymentalne w celu weryfikacji modelu. (Modelowanie wspinającego się robota z chwytającymi pazurami).

Keywords: Grasping claw; hook-like claw; wall climbing robot.
Słowa kluczowe: chwytający pazur, pazur hakowy, robot wspinający się.

1. Introduction

Bridges have been widely used throughout the world due to its good seismic resistance and economy. As the main component, the security of the tower attracts wide attention. At present, the tower and piers are mainly inspected manually. However, with the emergency of the large-span bridges, the testing cycle lasts longer and is becoming more dangerous and difficult. With the progress of the robot technology, the study of lightweight climbing robot to inspect the bridges automaticly is the new research orientation[1-2].

Traditional attachment methods are not suitable for climbing on the cracked or rough surfaces of the concrete, water brush stone and brick. A wall-climbing robot based on grasping claw is proposed in this paper, with the intent to overcome the above shortcomings. There have been some applied cases of climbing robot based on hook-like claw. Different attachment materials, including carbon nanotubes and polymer materials, were developed in Stanford University. Spinybot [3], a wall-climbing robot to imitate the wall-climbing mechanism of beetles was created. Having tiny barbs on its feet to hook onto the micro-protuberances on rough wall surfaces, the robot can scale concrete and brick surfaces. Using micro spines that catch on surface asperities, researchers proposed a spiny-based bio-inspired robot called RiSE, designed for scansorial environments [4]. Based on bionics, traditional design, and module combination, manufacturers build tree-climbing and ground-walking robots by combining six modules for legs. The shortcomings of these robots is the usage of numerous driving devices, which results in a complex mechanical structure. After studying the delicate structure, adhesion performance, and movement characteristics of gecko foot setae [6–7], Dai designed a gecko robot that can move freely in 3D space [8]. He also investigated the microstructure of the claws of hornets, beetles, and other insects to design bionic feet [9]. Sintov put forward a hook-like claw wall-climbing robot called CLIBO [5], which can remain on a rough wall surface in a fixed posture for long periods. CLIBO can be used in monitoring, rescue, observation, and entertainment applications.

The robots discussed above can hook onto the micro-protuberance on the rough wall surface under the action of gravity. However, there will be no generation of an attachment force pointing to the wall, so that the robot may be easily affected by high-altitude wind load and wall surface vibration. To overcome these shortcomings, the paper introduces an attachment scheme for the small claw.

First, the design method for grasping claw module is researched based on the interaction force between claw tip and the micro-protuberance on the rough wall surface. Then mechanical analysis is performed to formulate the design scheme of grasping-claw robot. Our study lays a foundation for the development of tower testing robot which has the advantages of small size, light weight and flexible movement.

2. Model of the climbing robot based on hook-like claws

Many animals with sharp claws, such as beetle and ants, can move freely on a rough surface; others like cockroach and grasshopper can easily attach to the surface of water brush stone. However, these animals can not stay on the smooth glass surface. Studies show that the tiny claw-shaped barbs on their feet can grasp the micro-protuberances on the wall. Apparently, the structure of the hook-like claws of these animals is an important factor for their climbing on the wall.

In this section, a wall-climbing robot model based on grab claw is built by modelling on the characteristic of claw grasping of wall-climbing animals, such as cockroach and beetle. To be specific, the robot is mainly used to detect cracks on the concrete surface of cable-stayed bridge tower and viaduct bridge piers in remote mountainous areas.

Driven model is shown in Fig. 1(a). Its principle can be described as follows: eccentric wheel mechanism is driven by a steering engine; a small roller is installed between pressure plate and hook-like claw, a torsion spring is placed on each hook-like claw. When the pressure plate is pressed downward, every hook-like claw stretches, and claw tip is separated from the micro-protuberances on the wall surface, deforming the torsion spring. When the pressure plate is drawn back, every hook-like claw grasps the wall surface independently under the driving by respective torsion spring. When a certain claw comes in contact with the micro-protuberances on the wall surface, the pressure plate will continue to draw back, while the tips of other sharp claw will continue looking for graspable micro-protuberances.

The distribution of the hook-like claws is displayed in Fig. 1(b). Two pairs of claws are arranged on the upper and lower parts of the module. To improve the stability of the robot, another pair of hook-like claws can be arranged on the left and right sides of the module, respectively. Torsion spring drives the independent movement of each hook-like claw, thereby increasing the reliability and probability of tight grasping of micro-protuberances on the wall surface.

In the climbing model, when the hook-like claw grasps the wall, the micro-protuberances on a rough wall surface provide the robot with an attachment force pointing towards the wall surface. The constraint by wall surface on the robot is increased, which helps to counter the wind load in high altitude and the adverse effect of wall surface vibration on the climbing performance of the robot.

3. Force analysis of grasping claws

The interactions between the grasping claws and wall surface are analysed. Cone-shaped micro-protuberance is selected to study the mechanical performance of the hook-like claw when grasping the surface micro-protuberances.
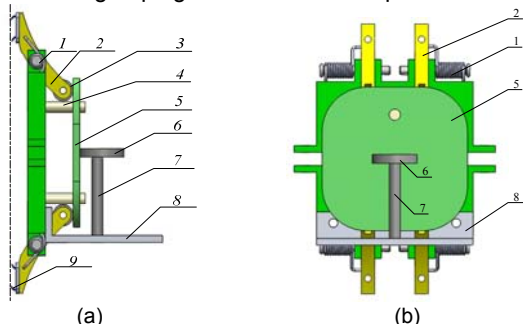

Fig. 1. Driven model of the torsion spring, 1-torsion spring, 2-hook-like claw, 3-roller, 4-guide pillar, 5-pressure plate, 6-eccentric wheel, 7-shaft, 8-motor fixed plate, 9-claw tip.

3.1. Force analysis of grasping claw module

According to the climbing models constructed in previous section, the stress on the hook-like claw is shown in Fig.2. The direction of friction F_{f2} on the lower claw tip is directly related to the magnitude of torque of torsion spring. When $M_2 > M_0$, F_{f2} points downward along the inclined plane of micro-protuberance; when $M_2 < M_0$, F_{f2} points upward along the inclined plane of micro-protuberance; when $M_2 = M_0$, $F_{f2} = 0$ is obtained. Here M_0 is the critical value of the torque of torsion spring.

According to the equilibrium conditions, we can obtain

(1) $$\begin{cases} F_{v1} = F_{v2} = FL/D \\ F_{s1} - F_{s2} = F \end{cases}$$

The torque of the torsion spring of the upper hook-like claw is

(2) $$M_1 = F_{s1} \times L_1 - F_{v1} \times (D/2 - L_2)$$

The torque of the torsion spring of lower hook-like claw is

(3) $$M_2 = F_{s2} \times L_1 + F_{v2} \times (D/2 - L_2)$$

To simplify the calculation, the angles of the upper and lower micro-protuberances are set to be equal, that is $\theta_1 = \theta_2 = \theta$, and $F_{f1} \cos\theta > N_1 \sin\theta$ for upper claw, thus $F_{f1} > N_1 \tan\theta$. Therefore, the angles of micro-protuberances must be smaller than the self-locking angle between claw tip and micro-protuberance, i.e. $\theta < \arctan(\mu)$, otherwise, the upper claw will slide away, and can not grasp the wall steadily.

By analysing of the contact points on the lower hook-like claws, the following can be obtained:

$$\sum M = (F_{f1}\cos\theta - N_1\sin\theta)D - FL = 0$$

After deriving the equation, we can get

(4) $$F_{f1} = N_1 \tan\theta + \frac{FL}{D\cos\theta} < \mu N_1$$

Here, N_1 and F_{f1} are the support force and friction exerted on the upper claw tip by the micro-protuberance; F_{s1} and F_{v1} are respectively the tangential and normal forces along the wall surface of the support force and friction exerted on the upper claw tip; N_2 and F_{f2} are the support force and friction exerted by the micro-protuberance on the lower claw tip; F_{s2} and F_{v2} are respectively the tangential and normal forces along the wall surface of the support force and friction exerted the lower claw tip. C is the center of mass of the hook-like claw, M_1 and M_2 are the torques of torsion spring for the upper and lower hook claws, θ_1 and θ_2 are the angle of the upper and lower micro-protuberances, F is the resultant force on upper and lower hook-like claws.

It can be seen from Eq. (4) that whether the self-locking of the upper hook-like claws will occur or not is related to the angles of micro-protuberances and the support force (torque of torsion spring) of the upper claw (Fig. 3). $S1$ is static friction curved surface of upper hook-like claw, and $S2$ is its sliding friction curved surface. It can be known that the smaller the angle of micro-protuberances, the larger the support force and static friction exerted on the upper hook-like claw will be. Also, the self-locking of the upper hook-like claw will occur more easily. When the angle of micro-protuberances is larger than a certain value, the static friction exerted on the upper hook-like claw will exceed the sliding friction. Then the hook-like claw will slide and cannot grasp steadily.

3.2 Analyzing of the hook-like claws

The direction of friction exerted on the lower claw tip is related to the magnitude of the torque of torsion spring (Fig. 2). Thus, we will analyse the stress on the hook-like claws under three different conditions.

(1) When $F_{f2} = 0$, i.e. when the torque of torsion spring reaches the critical value. Then the friction on the lower claw tip is zero. The balance equation can be obtained as follows:

(5) $$\begin{cases} F_{f1}\cos\theta - N_1\sin\theta = FL/D \\ N_2\sin\theta = FL/D \\ F_{f1}\sin\theta + N_1\cos\theta - N_2\cos\theta = F \\ F_{f1} \le \mu N_1 \end{cases}$$

After deriving from Eq. (5), we can obtain

(6) $$\begin{cases} N_1 = F\cos\theta + \frac{FL\cos^2\theta}{D\sin\theta} - \frac{FL}{D}\sin\theta \\ N_2 = \frac{FL}{D\sin\theta} \\ F_{f1} = F\sin\theta + 2FL/D\cos\theta \end{cases}$$
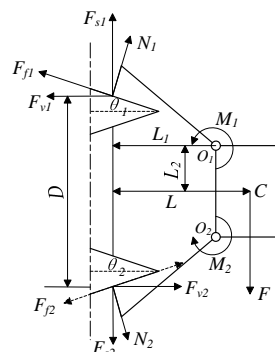

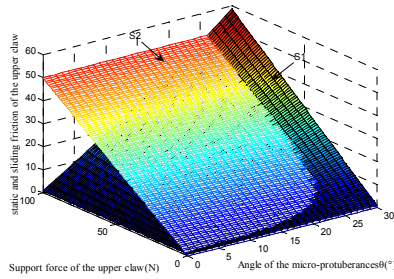Fig.2. Schematic diagram of stress on the hook-like claw
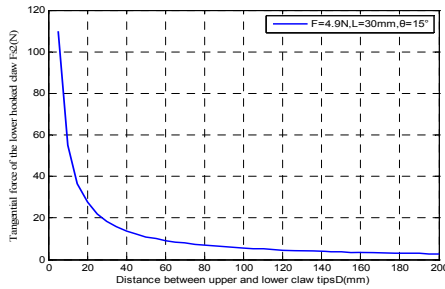
Fig. 3. Self-locking of upper hook-like claw

Fig. 4. Effect of distance between upper and lower tips on tangential force on lower claw

It can be known from Fig. 2 that the smaller F_{s2}, the steadier the grasping will be. Hence an appropriate D should be chosen to make F_{s2} as small as possible. $F_{s2} = N_2 \cos\theta = FL/D \cdot \cot\theta$, and its variation is shown in Fig. 4. We can see that the greater the distance between upper and lower claw tips, the more steady the grasping will be. This conclusion is also consistent with results from attachment model of insects on wall surface. However, as D increases，F_{s2} becomes increasingly smaller. Considering the size of hook-like claw module, we set the distance between upper and lower claw tips to be $D = 120mm$.

The relationship obtained from Eq. (6) between the stress exerted on upper and lower hook-like claws and the angle of micro-protuberances θ is shown in Fig 5. To maintain the balance of the hook-like claws, the static friction exerted on the upper hook-like claw must be smaller than its maximum static friction, thus $\theta \leq 18.4°$.

(2) The friction exerted on lower hook-like claw is pointing downwards along the inclined plane of micro-protuberance. When the torque of torsion spring is larger then the critical value, the corresponding force exerted on the hook-like claw is F, and the torque of torsion spring has a great impact on the hook-like claw, which tends to slide outwards along the micro-protuberance. When N_2 increases, its normal component along the wall surface increases too, that is, $N_2 \sin\theta > F_{v2} = FL/D$. Therefore, a friction pointing downwards along the inclined surface of the micro-protuberance is necessary to maintain the balance of the hook-like claws. Thus, we can get

$$\begin{cases} F_{f1}\cos\theta - N_1\sin\theta = FL/D \\ N_2\sin\theta - F_{f2}\cos\theta = FL/D \\ F_{f1}\sin\theta + N_1\cos\theta - N_2\cos\theta - F_{f2}\sin\theta = F \\ F_{f1} \leq \mu N_1, F_{f2} \leq \mu N_2 \end{cases}$$

1) When the upper hook-like claw slides, that is, $F_{f1} = \mu N_1$, we can get

$$(7) \quad \begin{cases} N_1 = \dfrac{FL}{D(\mu\cos\theta - \sin\theta)} \\ N_2 = \dfrac{FL\cos^2\theta + FL\mu\sin\theta\cos\theta}{D(\mu\cos\theta - \sin\theta)} - F\cos\theta + \dfrac{FL}{D}\sin\theta \\ F_{f1} = \dfrac{FL\mu}{D(\mu\cos\theta - \sin\theta)} \\ F_{f2} = \dfrac{FL\sin\theta\cos\theta + FL\mu\sin^2\theta}{D(\mu\cos\theta - \sin\theta)} - F\sin\theta - \dfrac{FL}{D}\cos\theta \end{cases}$$

The relationship of the forces exerted on the upper and lower hook-like claws to the angle of micro-protuberances θ (Fig. 6) can be obtained from Eq. (7). When $\theta \leq 18.4°$, $F_{f2} < 0$, which is impossible to occur in real situation, therefore, self-locking of upper hook-like claw occurs. When $18.4° < \theta < 26°$, the upper hook-like claw will slide, and the static friction exerted on the lower hook-like claw is smaller than the sliding friction, so the hook-like claws are kept in balance. However, the difference between these two values is so small that the hook-like claw is out of balance.

2) When the lower hook-like claw slides, that is, $F_{f2} = \mu N_2$, Eq. (8) will be obtained, The relationship of the forces exerted on the upper and lower hook-like claws to the angle of micro-protuberance θ (Fig. 7) can be obtained from Eq. (8). When the torque of torsion spring is larger than the critical value, the equilibrium state in which the lower hook-like claw slides will not occur.

Through integrating the two situations [1] and 2)], we can see that when the torque of torsion spring is larger than the critical value, that is, $\theta \leq 18.4°$, self-locking will occur. At this time, the greater the torque, the more steady the grasping will be.

$$(8) \quad \begin{cases} N_1 = \dfrac{FL\cos^2\theta + FL\mu\sin\theta\cos\theta}{D(\sin\theta - \mu\cos\theta)} + F\cos\theta - \dfrac{FL}{D}\sin\theta \\ N_2 = \dfrac{FL}{D(\sin\theta - \mu\cos\theta)} \\ F_{f1} = \dfrac{FL\sin\theta\cos\theta + FL\mu\sin^2\theta}{D(\sin\theta - \mu\cos\theta)} + F\sin\theta + \dfrac{FL}{D}\cos\theta \\ F_{f2} = \dfrac{FL\mu}{D(\sin\theta - \mu\cos\theta)} \end{cases}$$

(3) The friction exerted on lower hook-like claw pointing upwards along the inclined plane of micro-protuberance. When the torque of torsion spring is smaller than the critical value, the force F has a greater impact on the hook-like claw, compared with the torque of torsion spring. Then the lower hook-like claw tends to slide inward along the micro-protuberance. As N_2 decreases, its normal component along the wall surface also decreases, that is, $N_2 \sin\theta < F_{v2} = FL/D$. Therefore, a friction pointing upwards along the inclined plane of the micro-protuberance is necessary to keep the hook-like claws in balance. Thus,

$$\begin{cases} F_{f1}\cos\theta - N_1\sin\theta = FL/D \\ N_2\sin\theta + F_{f2}\cos\theta = FL/D \\ F_{f1}\sin\theta + N_1\cos\theta - N_2\cos\theta + F_{f2}\sin\theta = F \\ F_{f1} \leq \mu N_1, F_{f2} \leq \mu N_2 \end{cases}$$

When the upper hook-like claw slides, that is, $F_{f1} = \mu N_1$, we can get

$$(9) \quad \begin{cases} N_1 = \dfrac{FL}{D(\mu\cos\theta - \sin\theta)} \\[2mm] N_2 = \dfrac{FL\cos^2\theta + FL\mu\sin\theta\cos\theta}{D(\mu\cos\theta - \sin\theta)} - F\cos\theta + \dfrac{FL}{D}\sin\theta \\[2mm] F_{f1} = \dfrac{FL\mu}{D(\mu\cos\theta - \sin\theta)} \\[2mm] F_{f2} = -\dfrac{FL\sin\theta\cos\theta + FL\mu\sin^2\theta}{D(\mu\cos\theta - \sin\theta)} + F\sin\theta + \dfrac{FL}{D}\cos\theta \end{cases}$$

The relationship of the force exerted on upper and lower hook-like claws to the angle of micro-protuberances θ (see Fig. 8) can be obtained from Eq. (9). It can be got that when the torque of torsion spring is smaller than the critical value, the equilibrium state in which the upper hook-like claw slides will not occur.
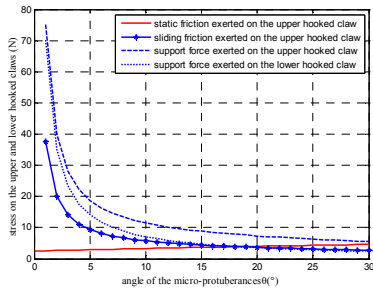

Fig. 5. Stress exerted on the hook-like claws when $F_{f2} = 0$
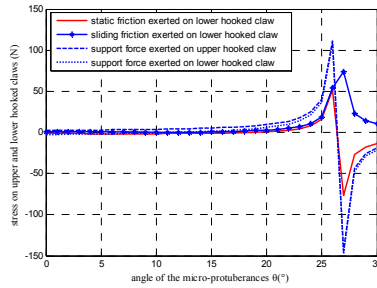

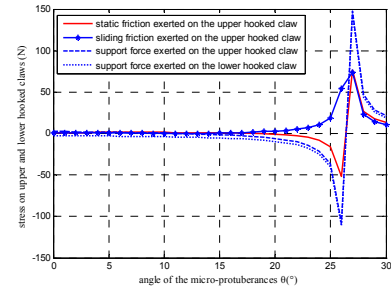Fig. 6. Stress exerted on the lower hook-like claws

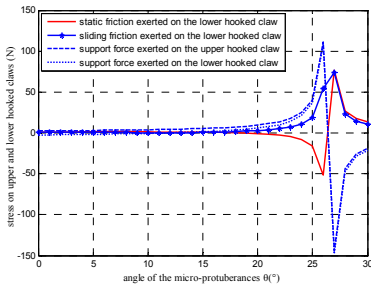Fig. 7. Stress exerted on the lower hook-like claws (b)

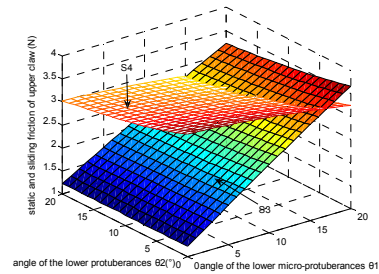Fig. 8. Stress exerted on the lower hook-like claws (a)

Fig. 9. Comparison between static and sliding friction exerted upper hook-like claw
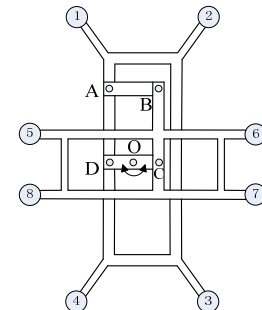

Fig. 10. Climbing model of the robot with eight feet.

3.3 Analysis

Through integrating these three situations [(1), (2) and (3) in last section] of friction exerted on the lower hook-like claw, we can conclude that, to achieve stead attachment of the wall-climbing robot on the wall surface, the angle of micro-protuberances is $\theta < 15.5°$. The minimum value of torque of torsion spring necessary to keep the hook-like claw in balance is thus obtained. The greater the torque, the more steady the grasping will be.

The above analysis is based on the situation in which the angles of upper and lower micro-protuberances are equal and the upper and lower claw tips grasp the micro-protuberances at a vertical angle. The offset distance between upper and lower claw tips is negligibly small in relation to the overall hook-like claw. In real situations, however, the angles between upper and lower micro-protuberances is different, that is, $\theta_1 \neq \theta_2$. So the sliding of the lower claw tip is a critical state of keeping the hook-like claw in balance. Thus, the equation can be concluded:

4. Inspection System

The main task of the robot designed in this study is carrying the detection equipments to test the tower of the cable-stayed bridges. Generally, the height of the main large-scale bridge tower is above 200 meters. The height of main tower of Sutong Bridge reaches 300m. Therefore, the bridge tower testing robot is a typical high-altitude operation robot. In this section, the system outline for testing robot prototype, gait planning and the overall function of the testing system are formulated according to the special environment of cable-stayed bridge.

$$\begin{cases} N_1 = \dfrac{FL}{D}\dfrac{\cos\theta_1\cos\theta_2 - \mu\cos\theta_1\sin\theta_2}{\sin\theta_2 + \mu\cos\theta_2} + F\cos\theta_1 - \dfrac{FL}{D}\sin\theta_1 \\[2mm] N_2 = \dfrac{FL}{D(\sin\theta_2 + \mu\cos\theta_2)} \\[2mm] F_{f1} = \dfrac{FL}{D}\dfrac{\sin\theta_1\cos\theta_2 - \mu\sin\theta_1\sin\theta_2}{\sin\theta_2 + \mu\cos\theta_2} + F\sin\theta_1 + \dfrac{FL}{D}\cos\theta_1 \\[2mm] F_{f2} = \dfrac{FL\mu}{D(\sin\theta_2 + \mu\cos\theta_2)} \end{cases}$$

Comparison between the static friction and sliding friction exerted on the upper hook-like claw can be seen in Fig. 9. $S3$ is the static friction curved surface, and $S4$ the sliding friction curved surface. It can be obtained that when $\theta < 15.5°$, the hook-like claws can grasp steadily. The smaller the angle of the upper micro-protuberances, the more steady the grasping will be. When the angle of upper micro-protuberances is a fixed value, the angle of lower micro-protuberances can vary within a relative large range.

4.1 System Outline

Tower inspection robots belong to a specialized group of mobile robots. Their main feature is their climbing ability versus the weight of the body and the resistance of the fissures. In a tower inspection robot system, the structural mechanism is the most critical component of the system as it directly affects capability and technical index. The designer should consider not only climbing methods, as is done in conventional mobile robots, but also safety characteristics such as anti-vibration and anti-wind load as

the robot works at high altitudes. During robot design, therefore, the following requirements should be taken into account:

(1) Mass of the robot is less than 4 kg, and with payloads below 1 kg. Travel speed: 0 to 0.08 m/s, and once charged, the robot can move over 500m;

(2) Payload capacity, which enables the robot to carry NDE equipment and CCD cameras or other devices;

(3) Operation efficiency, in which the climbing robot should efficiently navigate on the towers that are several hundred meters long;

(4) Complexity of the entire structure: the robot should be small and lightweight, and consume little energy.

Characteristics such as simple control options, convenience in carrying sensors, and overall costs are the other primary factors.

4.2 Climbing model of the robot with eight feet with four feet

On the basis of the mechanical models of interactions between the sharp claws and micro-protuberances, we design a model of the wall-climbing robot with eight feet. The principle underlying robot function can be described using a parallelogram mechanism [ABCD Fig.10]. Hook-like claw modules (1, 2, 3, 4) are connected to the rack of the parallelogram mechanism; hook modules (5, 6, 7, 8) are fixed onto the connecting rod of the parallelogram mechanism. These modules are driven by a steering engine as they grasp micro-protuberances on a wall. The main steering engine is installed at point O, driving the drive rod to swing back and forth within a predetermined angle range. The two sets of hook-like claws alternately move up and down, pushing the robot up the wall.

4.3 Gait planning for tower-climbing robot with four feet

Wall-climbing robot moves with a parallelogram mechanism (ABCD) as shown in Fig.11a. Hook-like claw modules(1, 2, 3, 4)are fixed onto the connecting rod of the parallelogram mechanism. The steering engine is installed at point O, driving the drive rod to swing back and forth within the predetermined range of angle. The two sets of hook-like claws move up and down alternately, and grab unto the micro-protuberances on wall surface to climb.
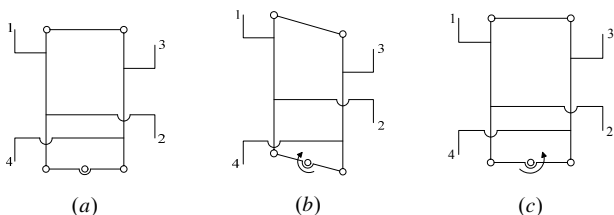

Fig. 11 Diagonal gait of the robot with four feet

The common gaits of the quadruped robot include diagonal gait, tripod gait, etc. Gecko supports its body and keeps balance with two legs in contact with the wall surface all the time as it climbs up the vertical wall. This paper designs a diagonal gait which imitates gecko crawling. The robot moves upwards twice within in one cycle. Fig. 11(a) shows the preparation stage of gait; Fig. 11(b) and Fig. 13 (c) show a gait cycle. In Fig. 11(b), hook-like claw module 1 and 2 stretches and the robot steps forward; hook-like claw module 3 and 4 grasp the micro-protuberances on the wall surface firmly. Supported by hook-like claw module 3 and 4, the robot completes its first movement. In Fig. 11(c), hook-like claw module 3 and 4 are stretches and the robot steps forward; hook-like claw module 1 and 2 grasp the micro-protuberances on the wall surface firmly. Supported by

hook-like claw module 1 and 2, the robot completes its second movement. The body posture of the robot is shown in Fig. 11(a). The first gait cycle completed, the robot enters the next gait cycle. The wall-climbing robot continuously moves upwards on the vertical wall by these gaits.

4.4 Diagram of the Inspection System

The schematic of the inspection robot system is shown in Fig. 14. The system is divided into three parts: a motion control system, a detecting system, and a monitoring system.

(1) Motion control system. This system includes climbing robot and a remote-control subsystem. The robot carries the inspection instruments and climbs on the walls. The moving state of the robot is controlled by the remote-control subsystem. Meanwhile, the motion parameters of the robot and the inspecting signals, such as moving velocity and index signals of surplus energy in the battery, are transferred to the remote monitoring centre on the ground.

(2) Detecting system. This system includes four CCD cameras, a signal synthesis card, and data memory. All of these are carried by the robot. After the videos and pictures are taken by the cameras, the signals are stored in the data memory. Meanwhile, these signals are transmitted to the ground monitoring system through a small transmitter.

(3) Ground monitoring system. This system is operated through a wireless transmission unit that includes two components: a small transmitter installed on the robot and a transceiver placed on the ground. Through the transceiver, operators can send out control commands, monitor the running state of the robot, and receive real-time videos of the wall surface. Meanwhile, through image processing technology, the degree to which the wall is damaged is obtained immediately after receiving the video.
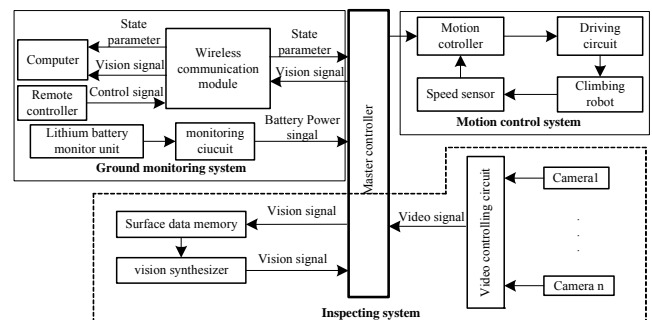

Fig. 14. Diagram of the inspection robot system

5 Conclusion

An innovative claw-based climbing model of wall inspection robot was developed in this paper. The design method for grasping claw is researched based on the interaction force between claw tip and the micro-protuberance on the rough wall surface. The results of mechanical analysis and simulation demonstrate that the claws can grasp the rough wall surface steadily. The study can be a foundation to develop a tower testing robot which can be applied to work on curved surface with large curvature, such as concrete wall surface, roof top and power poles.

REFERENCES
[1] Xu F. Y., Wang X. S., and Wang L., Cable Inspection Robot for Cable-Stayed Bridges: Design, Analysis, and Application. JOURNAL OF FIELD ROBOTICS, 28 (2011), No.3, 441-459

[2] Xu F. Y., Wang X. S., The Climbing Model and Obstacle-Climbing Performance of Cable Inspection Robot for Cable-stayed Bridge, Transactions of the Canadian Society for Mechanical Engineering, 35 (2011), No. 2, 269-289

[3] Asbeck A. T., Kim S., Cutkosky M. R., Scaling hard vertical surfaces with compliant microspine array, International Journal of Robotics Research, 25(2006), No. 12, 1165-1179

[4] Spenko M. J., Haynes G. C., Saunders J. A., Biologically Inspired Climbing with a Hexapedal Robot, Journal of Field Robotics, 25(2008), No. 4-5, 223-242.

[5] Avishai S., Tomer A., Amir S., Design and motion planning of an autonomous climbing robot with claws, Robotics and Autonomous Systems, 59(2011), No. 11, 1008-1019.

[6] Guo C., Wang W. B., Yu M., Dai Z. D., Great wall into account and unwebbed house lizard foot setae structure and adhesion properties of comparative study, Science in China Series C: Life Sciences, 37(2007), No.5, 568-574.

[7] Li H. K., Dai Z. D., Shi A. J., Big house lizard in the vertical and horizontal surfaces on the trot walking and joint angle observation, Chinese Science Bulletin, 53(2008), No.22, 2697-2703.

[8] DAI L. Q., ZHANG H., DAI Z. D., Analysis on Feet Workspace of Gecko Robot and Gait Planning for Its Coordinated Motion, Robot, 30(2008), No. 2, 182-186.

[9] X. W. GUAN, H. ZHANG, A. H. JI, Z. D. DAI, Development of claw-inspired foot structure for wall-climbing robot, Mechanical & Electrical Engineering Magazine, 26(2009), No. 2, 1-4.

Authors: Fengyu Xu, lecture, College of Automation, Nanjing University of Posts and Telecommunications, Nanjing, Jiangsu Province, China. E-mail: xufengyu598@163.com.